

ABSTRACT

This project aims to study the modal vibration characteristics of wings of a known aircraft model AIRBUS A380-800. A comparative study has been made using two methods; Finite Element Simulation, and Analytical Numerical approach using Rayleigh-Ritz approximation. The aim of this project is to validate or disprove the results of vibration analysis obtained from FEM ANSYS simulation with that of Numerical Method. The root air-foil profile is suspected to be a Supercritical series air-foil, the coordinates of which have been adopted from online air-foil plotter tool. Many wing structural details have been relaxed and suitable geometric assumptions have been taken in order to ease the process of result evaluation. Finally, it has been proved that the results from Rayleigh-Ritz approximation method are not in agreement with results from Finite element simulation through ANSYS modal analysis.

I. INTRODUCTION

The modal analysis of any structure experiencing vibration, especially transverse vibration gives us the vibrating frequency of each mode which that system undergoes progressively. A mode of vibration can be referred as a pattern of motion in which each component in the oscillating system produce similar sinusoidal motion with same frequency & fixed phase lag relations. In-case if the vibrating structure has its first resonant frequency as the rigid body mode itself, we would find that that frequency value is 0 Hz. But since an aircraft wing is not one continuous structure in real application, the rigid body frequency is normally not the first frequency met. Aircraft wings are usually thin-walled, non-uniform and discontinuous members which collectively make the wing look swept backward or in few specific cases, forward. Also, there are intermittent ribs and spars running across and throughout the wing which serves as the framework of the structure. On top of that, there are prime-movers, actuators and strainers and all other sorts of fuel handling mechanisms which are all essentially located inside the wing interior hollow spaces. A full-blown engineering simulation is thus limited by CAD model design challenges. Also, one would not be able to account for flow induced vibro-acoustic sound propagation and machine-produced vibrating effects on the wing without the help of proper probing tools and without replicating actual action of an object flying through the fluid medium (air). However, to consider the wing as a continuously running solid mass member is one allowable assumption. The aircraft wing under study is of Airbus A380-800. Being a proprietary technical information, Airbus is discreet about the type of air-foil series they are using. However, it is suspected to be from the Supercritical II series profiles, typically a blend of NASA SC(2) - 0610 for the root and NASA SC(2) - 0606 for the tip [1]. I have adopted the profile geometry; the x vs $y(x)$ coordinates of the air-foil contour from airfoiltools.com. As to the discussion above, there are three different models which can be assumed to represent as a wing in the analysis. They are; a 1D beam element, a 2D plate element, and a 3D solid element. The Euler-Bernoulli beam theory is the correct representation of the problem since we are assuming that our wing is a cantilevered beam under transverse vibration due to lateral air flow.

II. CAD MODEL DESCRIPTION

To make a 3D CAD model of the wing, we need to have air-foil contour coordinates. As mentioned before, the NASA SC(2) 0610 & 0606 is used directly by importing the coordinates as *.dat file* from airfoiltools.com. The figure below represents the profile section

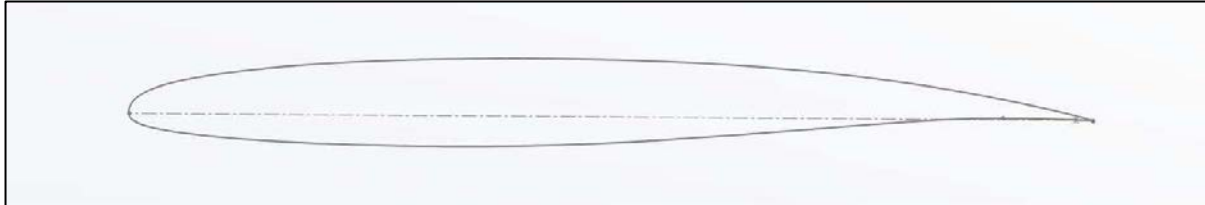


Figure 1. Air-foil contour of AIRBUS A380-800

Details about the air-foil characteristics are as follows;

- a.) **Max thickness** - 10 % of the mean chord-length 'c' at 38 % 'c' from the leading edge.
- b.) **Max camber** - 1.8 % of the mean chord-length 'c' at 82 % 'c' from the leading edge.

The 3D CAD model of the wing prepared is non-parametric and includes no aero-derivative information. The process to achieve such continuous looking solid wing form is laborious.

It either requires a parametric sweep relation of every guide curve that can be distinctively set-up for the leading edge, trailing edge, and trailing edge back-sweep angle. The standard engineering practice is to first create ribs and spars that support the frames and plates of the aircraft wing. Then to reduce the mass of those structures and make space for hollow cavity where other prime-movers will be fitted. And then, the outer panel frames are attached and extend till the tip according to how guide splines dictate. A standard wing of an Airliner has a dihedral angle already provided at the root of the wing which is attached to the wing box. This is done to give a pre-tension kind of effect so that when the aircraft actually starts to observe flutter in turbulent airflow, it performs better in the roll conditions and don't suffer excessive bending and/or limit-cycle oscillations.

The other method is to use the engineering drawing views already published by AIRBUS Aerospace Company and generate a precise 3D model from the outlines of 2D drawing. This is not a standard engineering practice though; however, it simplifies our analysis. The wing properties as outlined by AIRBUS A380-800 Aircraft characteristics manual are;

Table 1. List of geometric parameters that describe the wing

Parameter	Value	Parameter	Value
Wing Span	261.8 ft	Wing Sweep Angle	33.5 ° (backward)
Mean Length	239.5 ft	Taper ratio	0.26
Wing Area	9100 sq. ft	t/c ratio	0.08
Aspect Ratio	7.53	Mean Aerodynamic Centre location	60 % length from tip

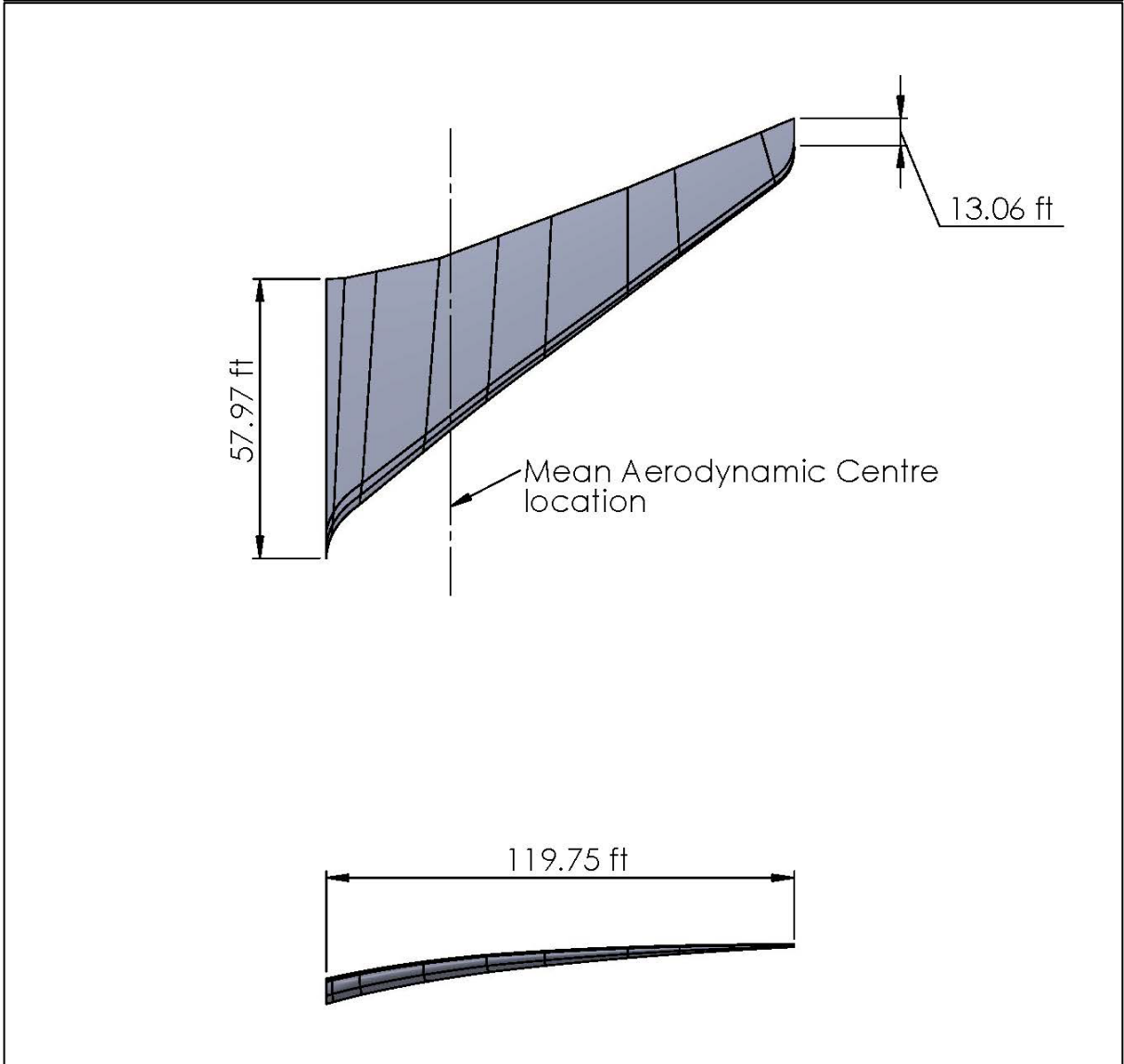
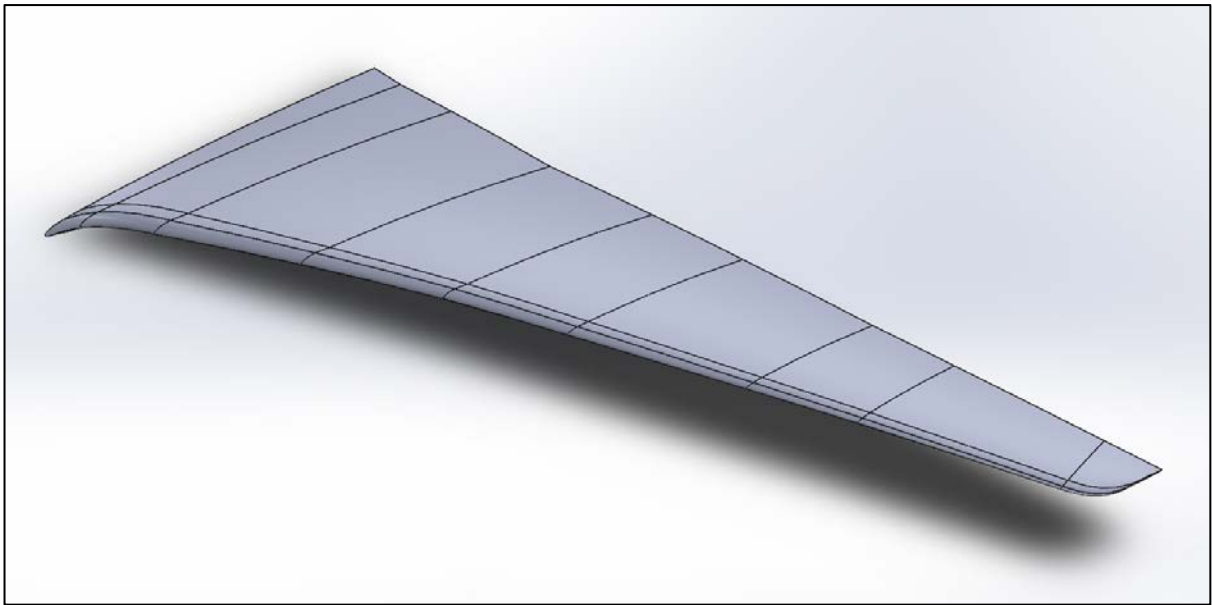


Figure 2. 3D CAD model precisely representing the wing of A380-800.

For each engineering analysis, the following material properties were assigned] for the wing;

Engineering Material	High Strength Aluminium <i>Alloy AL – 7075</i>
Material Density	79.5703 Kg/cu. ft
Youngs Modulus	71.78 GPa
Yield Strength S_{yt}	103 MPa

The 7075 – Aluminium Alloy is known for its use in high stressed application mainly because of its high ductility and good fatigue resistance characteristics. Thus, its main use in A380 is in airframe construction.

The discussion below will detail out the construction of this CAD model and will also show why it correctly represents the actual Airbus A380-800 wing with supercritical design.

- When not having parametric relations that can approximate splines or curves for the leading edge or trailing edge, we can make use of the Technical Drawings which contains front, and side profile of the wing.
 - In any commercial CAD package, we can start-off by selecting two intersecting planes. Typical choice of the planes be made according to the view which will be traced from the drawing.
 - For example, if the air-foil profile is required to be traced, then I should better draw it as a side-view rather than as a front view.
- Having made the choice of the planes, we now actually require an intersecting edge.
 - This is the edge where the two views of the part (side view and front view) intersect. Take again the example of the air-foil profile. At the leading-edge tip viewed from the side view, we will place the root region of the wing which is connected to the wing-box as seen from front, i.e. front view of the wing. But this front projected view will be aligned 90° upwards.
- Swivelling the planes, one will be able to clearly see how the wing's side view and front view gets spatially attached. The next task will be to mark a start point.
 - The start point is required because, it will help in initiating the tracing process of the curve. We will draw splines or straight lines as fit over the projected view from the drawing itself. This is sort of following the outline and making a new drawing.
 - The other curve to be traced is in other plane at a different orientation. It gives us a general imagination of how the component is going to get developed.
- For curves that can only be replicated by using the spline lines, one must take care that the curve is smooth. For that the curvature comb of the spline must be smooth and not abrupt at any place. The commercial package SolidWorks has a tool that monitors it well.
 - If drawing the upper surface of the air-foil, for example, use multiple points in between the start and end point. This is because a single start and end point will not possibly make the upper surface. Multiple points in-between will ensure the smoothness of the curve criteria.
- At the end, when all the profiles have been traced, we can use the leading edge & trailing edge splines as our guide curves for the profile sweep feature.

Following the above procedure is easily ridden with possibility of dimensional errors since the curve accuracies cannot be commented. However, after the 3D CAD model has been made, we can make a quick check of the model. Since we are aware that A380-800 has a supercritical wing profile, we can validate whether our model will be performing as a supercritical air-foil or not. A supercritical air-foil profile is a strategic design that ensures that the wave drag onset is delayed when in transonic speed range. A Computational fluid dynamics simulation may validate our model.

To have a better understanding, I have made use of ANSYS CFD Post to analyse flow dynamics. For this, the Spalart-Allmaras viscous model which employs RANS; short for Reynolds-Averaged Navier-Stokes Equation method which requires only 1 equation to be solved [2]. The transonic flight speed of about 0.89 Mach (302.6 m/s) are more characteristic of this aircraft at its maximum cruise altitude of 43,000 feet. With the use of a supercritical air-foil, we must be able to see a shock region getting induced at near the tail-section which will be indicative of supercritical profile design. The mesh that was generated had 177692 tetrahedral elements constructed by 45345 nodes.

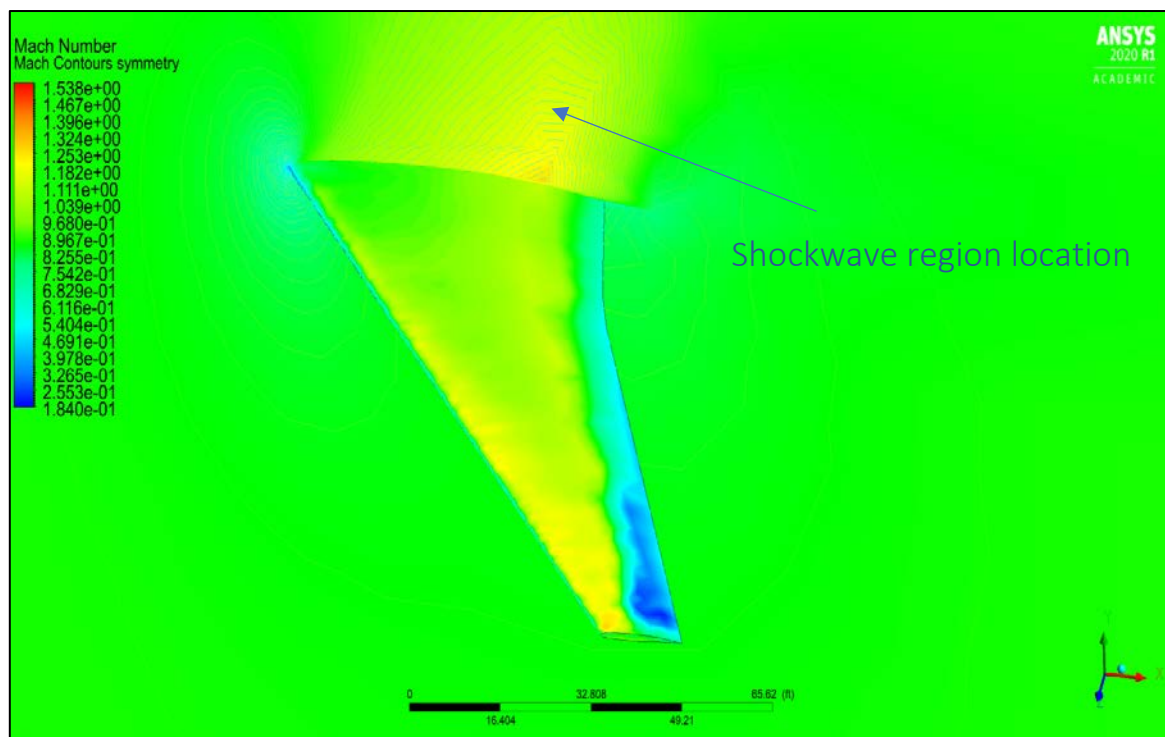
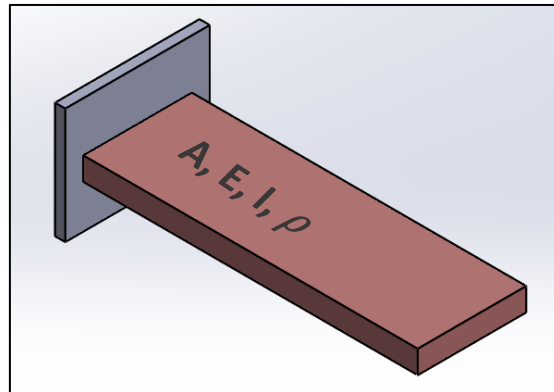


Figure 3. CFD analysis using CAD model displaying supercritical properties of the air-foil

That small red-yellowish peak formed at the root of the wing suggests the location of region where the MACH number of the flow is 1 due to the selected Critical Mach number of 0.89. This CFD result also gives one interesting observation, that towards the tip of the wing, the flow is merely subsonic and there is flow separation surface observed. And the leading edge towards the tip of the wing is having near-sonic conditions. These characteristics are guaranteed by the nature of supercritical air-foil profile. Hence, this result serves as partial validation that our 3D CAD Model is depicting the characteristics of the A380-800's wing form.

III. FEA METHODOLOGY

The finite element discretization will break the continuous beam of our wing into several decoupled systems. It becomes easy to translate the boundary conditions, dynamic conditions and transient responses of the wing into end effect, which is to observe the pattern of vibration. Here I have used ANSYS's Modal analysis toolbox to analyse the continuous system undergoing free vibration. ANSYS at its background uses Euler - Bernoulli's theorem to solve for the modal frequencies of the system under transverse vibration.



For a simple cantilever beam as shown above, the natural frequency can be found out by the formula [3, p. 536]:

$$\omega_n = (\beta_n L)^2 \sqrt{\frac{EI}{mL^4}}$$

where, ω_n (RPM) is the natural frequency of the oscillation at different modes of vibration;

I (lbm.ft²) is the Moment of Inertia in the x – direction;

$\beta_n L$ are the dimensionless weighted natural frequencies which are different for different boundary conditions (at the ends) of the vibrating member.

The Modal Analysis toolbox in ANSYS requires only a few assignments after which it can simulate the real vibration motion, hence showing us procedure to obtain the mode shapes and consequently the modal frequencies are as follows;

- Our CAD model requires to be assigned material properties which will mainly be the Young's Modulus, the Poisson's ratio, and the density. The material 7075 Aluminium alloy is not readily available in the ANSYS's material library. Hence it needs to be defined in the Materials library with all its structural and thermal properties value.
- After defining the materials in the library, we need our 3D CAD model to be imported in the setup of the Model Analysis modeler. We must ensure beforehand that our dimensions are in feet, the same units of dimension that our CAD model has. Not setting the units beforehand might only bring error in scaling of our mode shape frequencies, although not altering its exact values.
- An important step is to make the model realize the boundary conditions. Since its our assumption that the wing will behave as a cantilever, we are fixing the root-end of the

wing, thus constraining it's all 6 D.O.Fs. Now that we have fixed one end, we must assign our newly created 7075 – Aluminium Alloy material again to the CAD model in the set-up before we can jump to meshing of the model.

- And now we must mesh the model with default settings that the ANSYS processor suggests. We may refine the meshing to achieve more finer answer, however it's a redundant step.
- Having done the meshing step, we can go to the solutions tabs and press 'solve all'. This will generate a set of frequencies which will be visible at the centre-bottom part of the result screen. We can head straight there and select all the frequency bars and ask it to give a modal report.
- Thus, we now have a set of frequencies along with a movement pattern which simulate the motion of the member under that frequency. We only concern ourselves with first 3 modes of vibration. Though, in practice, the aircrafts never observe their second or third modal frequency in their operational life.

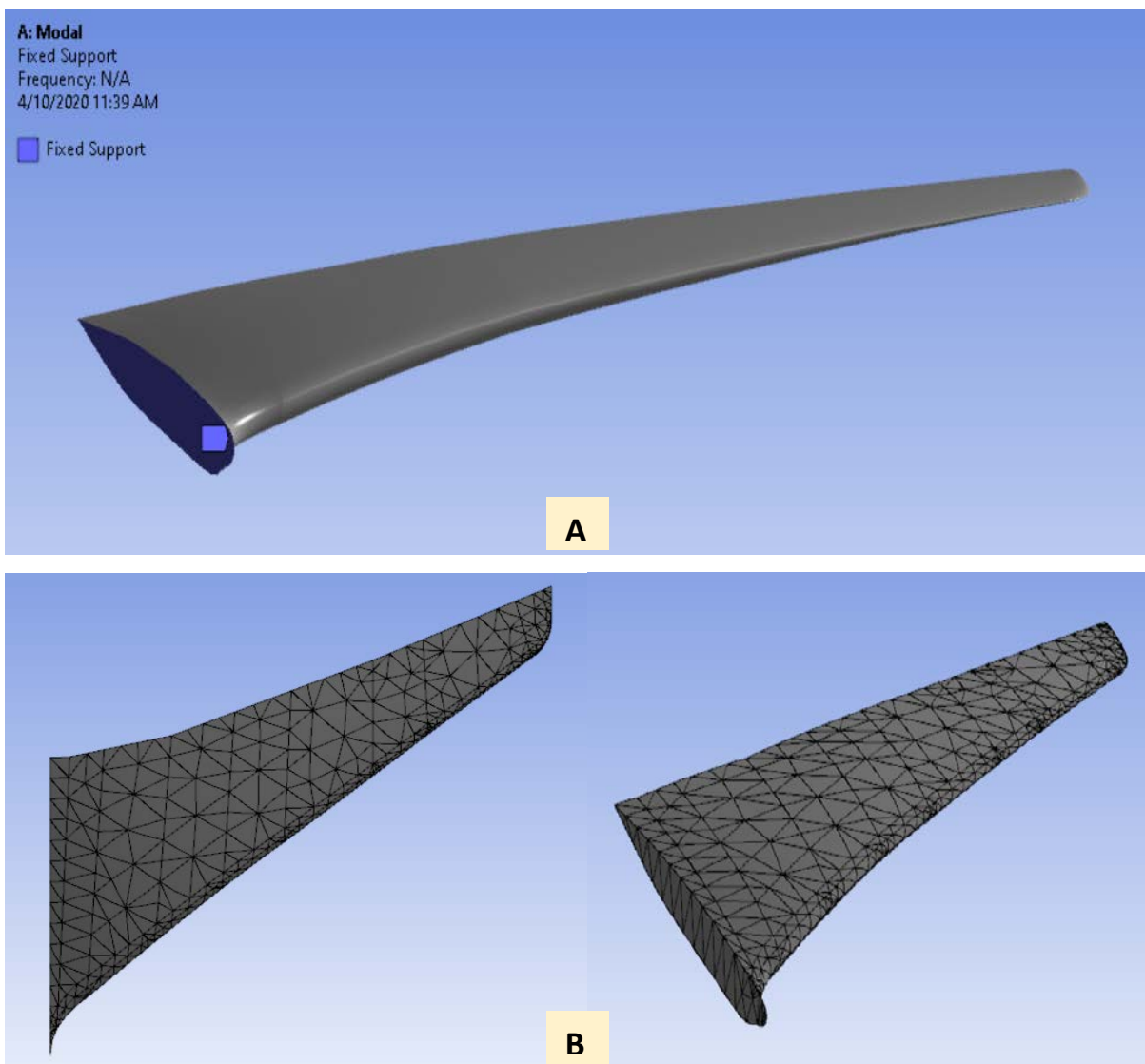


Figure 4. Fixed boundary at the root of the wing (A), Meshed model (B)

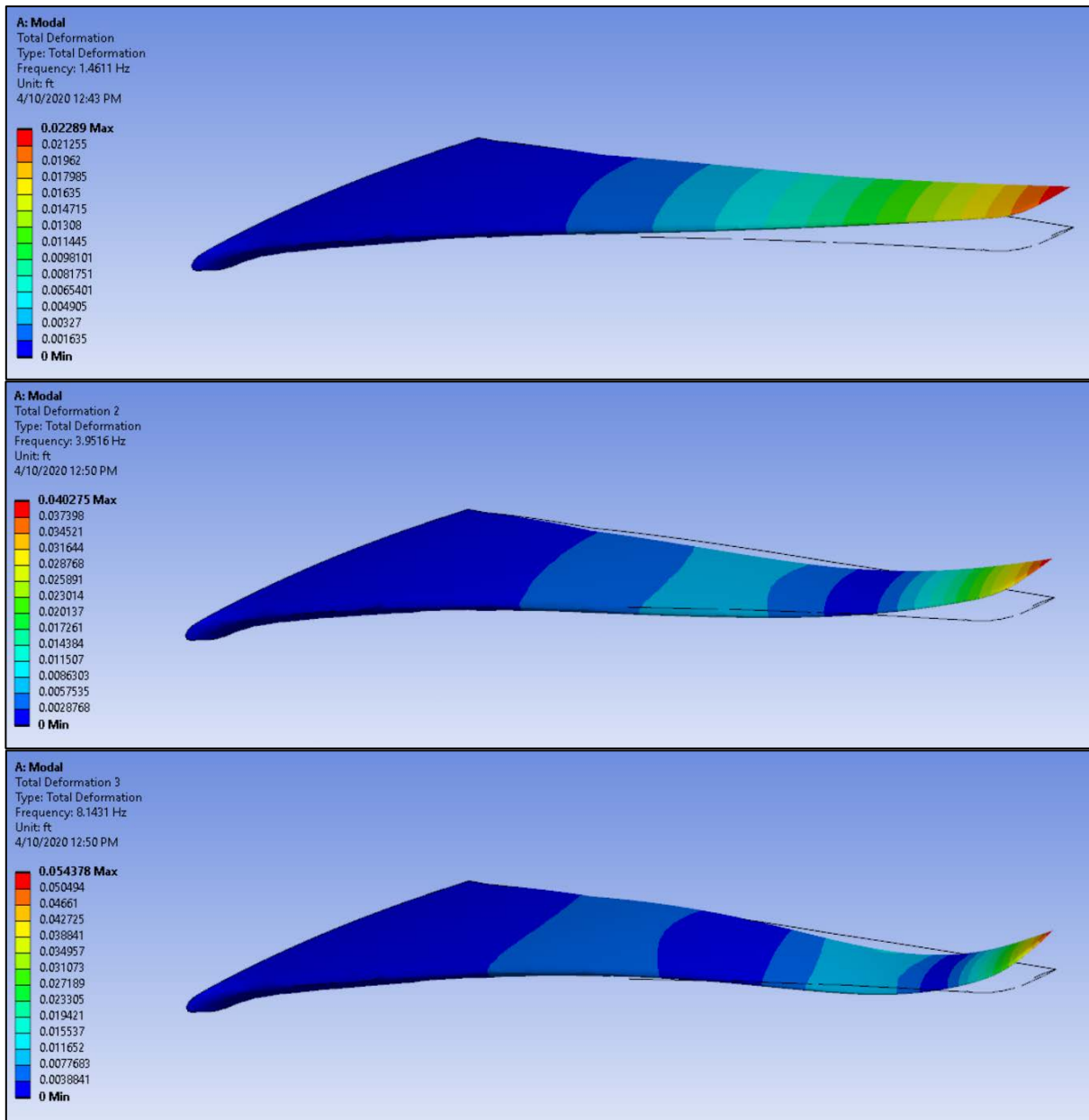


Figure 5. 1st, 2nd, 3rd modal frequencies pictured as displacement from mean position

The first three frequencies are;

$$f_1 = 1.4611 \text{ Hz,}$$

$$f_2 = 3.9516 \text{ Hz,}$$

$$f_3 = 8.1431 \text{ Hz.}$$

- In all three images, we see that according to the deformation contour chart, the region near the root of the wing observes lowest stress due to total deformation. This result verifies with the actual flight wing performance. In the actual flight conditions, there is very less structural deformation of the wing near the root region. All the aircraft wings have a region up-to certain length along its span that produces or contributes maximum lift. This region is located at ~ 35 - 40 % of span length from the root. Up-to this length, stresses remain almost negligible as can be depicted by the FE model above.
- Another important phenomenon: Aeroelastic flutter is apparent at near the tip of the wing. It is the self-excited structural vibration which depends on flexural rigidity of the wing.

IV. RAYLEIGH-RITZ APPROXIMATION METHOD

The previous two methods relied on Euler-Bernoulli's beam theory to perform modal calculations. Euler-Bernoulli's beam theory uses system's eigen functions to map the deflection and applied load in terms structures flexural rigidity. The Rayleigh-Ritz approximation method is different in that it uses energy-based modelling which uses calculus of variation given by Brachistochrone problem. This method makes use of Admissible shape functions / Trial functions which are defined different for different problems by the user [4, p. 794]. This is a sort of Finite element problem which can handle mixed system components having arbitrary shape and loading patterns.

IV.A Methodology

To derive the equation of motion using energy principle, the calculus of variation is applied first on a basic arbitrary volume V_s which undergoes small displacement in response to external applied forces.

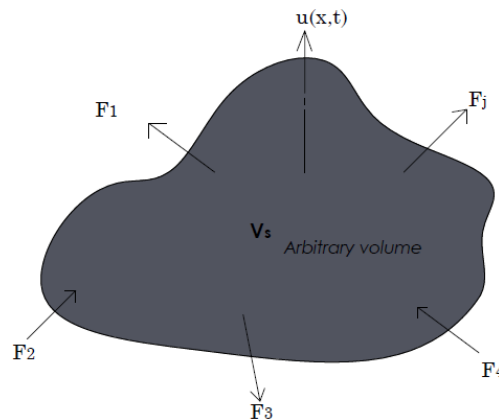


Figure 6. Arbitrary volume having applied forces on it.

Here, $\underline{u}(x,t)$ = displacement vector of location x at time t .

F_j = generalized applied forces on the object

The **Potential energy (U)** and **Kinetic Energy (T)** of the system is given by the formula [5, pp. 714, 715];

$$U = \frac{1}{2} \int_{V_s} \underline{S}^T \{C_s\} \underline{S} dV_s$$

$$T = \frac{1}{2} \int_{V_s} \rho \underline{\dot{u}}(x,t)^T \cdot \underline{\dot{u}}(x,t) dV_s$$

Where, \underline{S} is the Strain vector written as a column, C_s is the Elastic moduli matrix, $\underline{\dot{u}}(x,t)$ is the displacement rate vector, ρ & V_s are the density and volume of the arbitrary shape, respectively.

Applying variational calculus to express External work W_{ext} due to External forces f_j ;

$$\partial W_{ext} = \sum_{j=1}^j f_j \cdot \delta \underline{u}(x_j, t)$$

We can express strain in the volume as the function of displacement given by;

$$\underline{S}(x,t) = [L_u] \cdot \underline{u}(x,t)$$

Where, L_u is the operator that performs spatial derivatives and relates displacements to strains.

Since our displacement is in terms of x & t , we can split it using separation of variables method and write it as a series solution with product of two separate variables $\underline{u}(x,t) = \sum N_r(x) \cdot \underline{r}(t)$ [5, p. 714]. Here, $\underline{r}(t)$ is a time-based mechanically generalized coordinate, & $N_r(x)$ is the positional function, also called as Set of admissible shapes functions. These admissible shape functions/trial functions have to satisfy a list of conditions [6, p. 35];

- The boundary conditions must be incorporated in the set by the shape function.
- The shape functions must be a linearly independent set.
- They must be $m-1$ times differentiable where m is the highest order derivative given in L_u matrix.

To ensure completeness in the solution, the shape functions must form a complete set. For our case which is a fixed-free end condition, the mode shape equation that satisfies the solution is given by [3, p. 536];

$$N_r = A_1 \cos \beta_n x + A_2 \sin \beta_n x + A_3 \cosh \beta_n x + A_4 \sinh \beta_n x .$$

The n represents number of admissible shape functions included in the set. When substituted the $\underline{u}(x,t)$ in the equation of strain, we get;

$$\begin{aligned} \underline{S}(x,t) &= [L_u] \cdot N_r(x) \cdot \underline{r}(t) \\ &= B_r(x) \cdot \underline{r}(t) \end{aligned}$$

The $B_r(x)$ consists of the 1st derivatives of the shape functions. Plugging-in above relations, we have the potential energy as;

$$U = \frac{1}{2} \int_{V_s} \underline{r}(t)^T B_r(x)^T \{C_s\} B_r(x) \cdot \underline{r}(t) dV_s$$

Since, here the separated variable $\underline{r}(t)$ is not dependent on volume of the structure, it can be pulled out of the equation. Therefore, the potential energy is rearranged to;

$$U = \frac{1}{2} \underline{r}(t)^T \cdot \left[\int_{V_s} B_r(x)^T \{C_s\} B_r(x) dV_s \right] \cdot \underline{r}(t)$$

Similarly, Kinetic energy is; $T = \frac{1}{2} \dot{\underline{r}}(t)^T \cdot \left[\int_{V_s} \rho N_r(x)^T \cdot N_r(x) dV_s \right] \cdot \dot{\underline{r}}(t)$

In the above pair of equations, the bracketed terms are structure's stiffness and mass matrices, respectively.

We can also express the external work in terms of generalized forces as;

$$\begin{aligned} \partial W_{ext} &= \sum_{j=1}^j \delta \underline{u}(x_j, t)^T \cdot \underline{f}_j \\ &= \delta \underline{r}(t)^T \cdot \sum_{j=1}^j N_r(x_j)^T \cdot \underline{f}_j \end{aligned}$$

This can be simply expressed in the form of multiplication of vectors up-to ' j ' terms. This is expressed as given below.

$$= \underbrace{\begin{bmatrix} N_r(x_1)^T & N_r(x_2)^T & N_r(x_3)^T & \cdots & N_r(x_j)^T \end{bmatrix}}_{B_f} * \begin{bmatrix} f_1 \\ f_2 \\ f_3 \\ \vdots \\ f_j \end{bmatrix}$$

Let the matrix that contains transpose of the shape functions in column be noted as ' B_f '.

Therefore, the variational work can be written as $\delta W_{ext} = \delta \underline{r}(t)^T \cdot B_f \cdot \underline{f}$ after replacing the matrix with B_f .

Our final step is to deduce the equation of motion since our energy terms are now ready. Therefore, we can easily utilize the Lagrange's Method of first kind to substitute the displacement relationship in terms of mass and stiffness of the system [5, p. 714]. It is given by;

$$\frac{d}{dt} \left(\frac{\partial L}{\partial \dot{r}_i} \right) - \frac{\partial L}{\partial r_i} = Q_i \quad \text{(Here, } Q_i = \frac{\partial W_{ext}}{\partial r_i} \text{)}$$

Where, $L = T - U$, is called the **Lagrangian**. And the function Q_i comprises of all the external or non-conservative forces on the system.

The system that we derived is of the form of equation of motion that is familiar to us. The only difference is that the generalized coordinate is a time dependent and not space dependent. In the equation below, M_s & K_s are dynamic beam mass and stiffness matrices.

$$M_s \ddot{\underline{r}}(t) + K_s \underline{r}(t) = B_f \cdot \underline{f}(t)$$

IV.B Extension to our problem

Using the strategy described above, we now convert it into our problem at hand. Since the aircraft wing in simple terms represents a fixed-free boundary condition, let us refer back to the simple cantilever beam model to understand the material deflection and strain directions. The beam is assumed to have isotropic material strain characteristics.

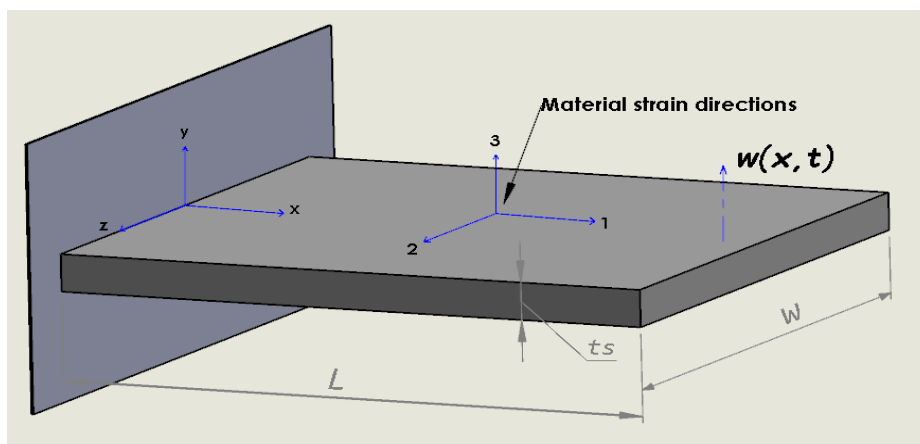


Figure 7. Cantilever beam showing material deflection & strain directions

Let us define the material deflection in 1,2,3 direction of the structure and relate it to the corresponding strain;

$$\text{Material deflection vector, } \underline{u}(x,t) = \begin{bmatrix} u_1(x,t) \\ u_2(x,t) \\ u_3(x,t) \end{bmatrix}$$

We are interested in the analysing the transverse vibration of the cantilever beam. Therefore, from the figure, we see that the transverse vibration is indicated by $w(x,t)$. We can relate this transverse vibration to the material deflection in that axis direction given by $w(x,t) = u_3(x,t)$. And using Euler-Bernoulli Beam theory, we can also relate deflection & strain in one direction to the deflection & strain in the other direction.

$$u_1(x,t) = -y \cdot \frac{d u_3(x,t)}{dx}$$

Therefore, strain being the first derivative of displacement is given by;

$$S_1 = \frac{d u_1(x,t)}{dx} = -y \cdot \frac{d^2 u_3(x,t)}{dx^2}$$

Strains of the other two directions are related by poisons ratio ν . Assuming the material is isotropic, the strain vectors can be represented in the matrix notation as;

$$\begin{bmatrix} S_1(x,t) \\ S_2(x,t) \\ S_3(x,t) \\ \vdots \\ \vdots \\ S_6(x,t) \end{bmatrix} = \begin{bmatrix} 0 & 0 & \left(-y \frac{d^2}{dx^2}\right) \\ 0 & 0 & \left(\nu y \frac{d^2}{dx^2}\right) \\ 0 & 0 & \left(\nu y \frac{d^2}{dx^2}\right) \\ 0 & 0 & 0 \\ 0 & 0 & 0 \\ 0 & 0 & 0 \end{bmatrix} * \begin{bmatrix} u_1(x,t) \\ u_2(x,t) \\ u_3(x,t) \end{bmatrix}$$

The strain terms S_1, S_2, S_3 relate to longitudinal strains in 1,2,3 coordinate directions described in the figure. The strain terms S_4, S_5, S_6 relate to shear strains in the structure. The central matrix which we find above is the differential operator matrix in which all the terms are 0 except three terms. The reason is that since we are interested to determine strains in all the directions in terms of displacement in transverse direction u_3 , we have neglected all other expressions. Therefore, we can have the following simplification;

$$\begin{bmatrix} u_1(x,t) \\ u_2(x,t) \\ u_3(x,t) \end{bmatrix} = \begin{bmatrix} 0 \\ 0 \\ \sum_{i=1}^N \phi_i(x) \cdot r_i(t) \end{bmatrix}$$

Here, we have chosen to denote shape function with symbol ϕ_r instead of N_r . And $r(t)$ continues to be the generalized coordinate. The shape function contains N number of terms, hence it forms a $3 \times N$ matrix here;

$$\phi_r(x) = \begin{bmatrix} 0 & \dots & \dots & \dots & 0 \\ 0 & \dots & \dots & \dots & 0 \\ \phi_1(x) & \dots & \dots & \dots & \phi_N(x) \end{bmatrix}$$

\downarrow \downarrow
 1st beam mode shape Nth beam mode shape

Now, we define the B_r matrix for our case;

$$B_r = L_u \cdot \phi_r(x) = y * \begin{bmatrix} \frac{d^2 \phi_1(x)}{dx^2} & \dots & \dots & \frac{d^2 \phi_N(x)}{dx^2} \\ -\nu \cdot \frac{d^2 \phi_1(x)}{dx^2} & \dots & \dots & -\nu \cdot \frac{d^2 \phi_N(x)}{dx^2} \\ -\nu \cdot \frac{d^2 \phi_1(x)}{dx^2} & \dots & \dots & -\nu \cdot \frac{d^2 \phi_N(x)}{dx^2} \\ 0 & \dots & \dots & 0 \\ 0 & \dots & \dots & 0 \\ 0 & \dots & \dots & 0 \end{bmatrix}$$

Now we can define our mass and stiffness matrices since all the elements necessary to define them are ready.

- The mass matrix is then defined as [5, p. 715];

$$M_s = \rho_s \int_{V_s} \phi_r(x)^T \cdot \phi_r(x) dV_s$$

With integration limits; $M_s = \rho_s \int_{-t_s/2}^{t_s/2} \left(\int_{-w/2}^{w/2} \int_0^L \phi_r(x)^T \cdot \phi_r(x) dx dz \right) dy$

- And the stiffness matrix is defined as [5, p. 715];

$$K_s = \int_{V_s} B_r(x)^T \cdot C_s \cdot B_r(x) dV_s$$

With integration limits; $K_s = E_s \int_{-t_s/2}^{t_s/2} \left(\int_{-w/2}^{w/2} \int_0^L B_r(x)^T \cdot B_r(x) dx dz \right) dy$

Here, the elastic moduli matrix C_s is essentially a scalar E_s since our problem is having the isotropic material. The limits of integration in y & z directions are applied in-view from centroidal plane occurring at Mean Aerodynamic chord length from the root of the wing. However, the integration limit for x direction should include the whole span of the wing.

Now we can plug the ϕ_r and B_r matrices in the dynamic mass and stiffness equations. We obtain the following forms for the mass and stiffness matrix;

$$M_s = \rho_s \int_{-t_s/2}^{t_s/2} \int_{-w/2}^{w/2} \int_0^L \begin{bmatrix} \phi_1(x) \cdot \phi_1(x) & \cdots & \phi_1(x) \cdot \phi_N(x) \\ \vdots & \ddots & \vdots \\ \phi_N(x) \cdot \phi_1(x) & \cdots & \phi_N(x) \cdot \phi_N(x) \end{bmatrix} dx dz dy$$

$$K_s = E_s \int_{-t_s/2}^{t_s/2} \int_{-w/2}^{w/2} \int_0^L y^2 \cdot \begin{bmatrix} \left(\frac{d^2 \phi_1(x)}{dx^2} \cdot \frac{d^2 \phi_1(x)}{dx^2} \right) & \cdots & \left(\frac{d^2 \phi_1(x)}{dx^2} \cdot \frac{d^2 \phi_N(x)}{dx^2} \right) \\ \vdots & \ddots & \vdots \\ \left(\frac{d^2 \phi_N(x)}{dx^2} \cdot \frac{d^2 \phi_1(x)}{dx^2} \right) & \cdots & \left(\frac{d^2 \phi_N(x)}{dx^2} \cdot \frac{d^2 \phi_N(x)}{dx^2} \right) \end{bmatrix} dx dz dy$$

The matrices above deliver overall property of the structure by including effects from discrete elements that these N shape functions divide it into. These matrices being N dimensional becomes difficult to compute by hand. Hence, we must utilize symbolic integration solver to obtain the multiplication results.

We can choose to have an optional simplification in our calculation which is in relation to orthogonality of shape functions. We must realize that the mode shapes of have an arbitrary scale of representation. And often the shape functions selected to represent a beam are orthogonal, therefore, we can select the scaling factor such that [3, p. 538];

$$\int_0^L \phi_i(x) \cdot \phi_j(x) dx = \delta_{ij} = \begin{cases} 0; & i \neq j \\ 1; & i = j \end{cases}$$

This would mean that the on-diagonal elements would simply become 0. The only elements that would remain would be on the off-diagonal. This simplification would be equally effective, the only difference would be that the solution would need to include a greater number of terms in-order to converge to the result.

Since our case study is on free-vibration characteristics, we must equate the modal equation to zero by considering the Force input absent. That is $M_s \ddot{r}(t) + K_s r(t) = 0$.

Having the M_s and K_s terms ready, we can obtain the ratio of stiffness to mass which is essentially the circular frequency squared (Rayleigh's quotient), given by the formula;

$$\omega^2 = \frac{K_s}{M_s}, (\text{rad/sec})^2$$

A reasonable question is that why would any selected shape function make the results ultimately converge. The explanation for it lies in the error minimization approach that is offered by Brachistochrone Problem. The inclusion of large number of terms in the formulation minimizes the error between true result and the arrived result.

Our point of study was vibrational displacement that the structure is undergoing in the transverse direction. For that we have chosen $w(x,t)$ which we again broke down to product of two distributed parameters system; $u(x,t) = \phi_r(x) \cdot r(t)$. With the above formulation, we also need to supply a few more details which are essential information to solve a problem involving Distributed Parameters System. Those are 'weighted natural frequencies' $\beta_n l$ and 'mode shape coefficients' σ_n , which are specific for particular boundary-condition type. With increasing number of terms in the shape functions, the values of these terms either become '1' or a direct multiple of that number of terms in the shape function. The table list down the weighted frequency and coefficient values below;

Table 4. $\beta_n l$ & σ_n values for $N = 1$ to 5 and $N > 5$ for a fixed-free beam condition [3, p. 539]

	N = 1	N = 2	N = 3	N = 4	N = 5	N > 5
$\beta_n l$	1.875104	4.694091	7.854757	10.995540	14.137168	$(2N - 1)\frac{\pi}{2}$
σ_n	0.7341	1.0185	0.9992	1.0000	1.0000	1.0000

Additionally, we must also define what shape function or mode shape equation we are going to use. The shape function needs to be assessed at two known boundary conditions; $\phi_r(0) = 0$ & $\phi_r'(0) = 0$. Putting these set of Boundary conditions will lead us to;

$$\phi_r(x) = A_1 (\cos \beta_n x - \cosh \beta_n x) + A_2 (\sin \beta_n x - \sinh \beta_n x)$$

Where, A_1 and A_2 needs to be calculated by factoring in another set of boundary conditions which looks after balancing the force and moment equilibrium conditions on the structure. For fixed-free boundary condition (a cantilever), the coefficients A_1 and A_2 are '-1' & ' σ_n '. Hence, our shape function equation becomes [3, p. 539];

$$\phi_r(x) = (\cosh \beta_n x - \cos \beta_n x) + \sigma_n (\sinh \beta_n x - \sin \beta_n x)$$

We must also learn where the values of σ_n came from. For our known cantilever beam boundary conditions, the formula to find the mode shape coefficient would be [3, p. 540];

$$\sigma_n = \frac{\sinh \beta_n l - \sin \beta_n l}{\cosh \beta_n l + \cos \beta_n l}$$

Using MATLAB symbolic computation, we can replicate the above theory and determine the modal frequencies of the simplified approximated structure. The detailed MATLAB script used to perform the calculation has been attached in the appendix section. The following frequencies were determined from the analytical method using MATLAB computation;

Table 3. 1st, 2nd, 3rd frequency for different number of terms included in shape function

freq	Values (Hz)							
	N = 3	N = 4	N = 5	N = 6	N = 7	N = 8	N = 9	N = 10
f_1	1.6035	1.6035	1.6035	1.6035	1.6035	1.6035	1.6035	1.6035
f_2	10.0488	10.0488	10.0488	10.0488	10.0488	10.0488	10.0488	10.0488
f_3	28.1377	28.1376	28.1376	28.1371	28.1370	28.1369	28.1369	28.1368

It is a general observation that upon increasing the number of contributing terms in shape function, the accuracy of the result improves. From the table above, we can observe that the first and second frequency values remains same throughout iterations, however, we can identify the third frequency converging to true value as a greater number of terms in the trial function are incorporated. But how should we know that the results have converged to a greater degree. We can have that indication from plotting a convergence analysis plot. Since the first and second frequency values are remaining stable throughout the iteration cases, we must only consider the 3rd frequency. In the graph, we would be able to observe from the trend-line that value of the frequency starts to plateau. That is when we realize that our results have converged.

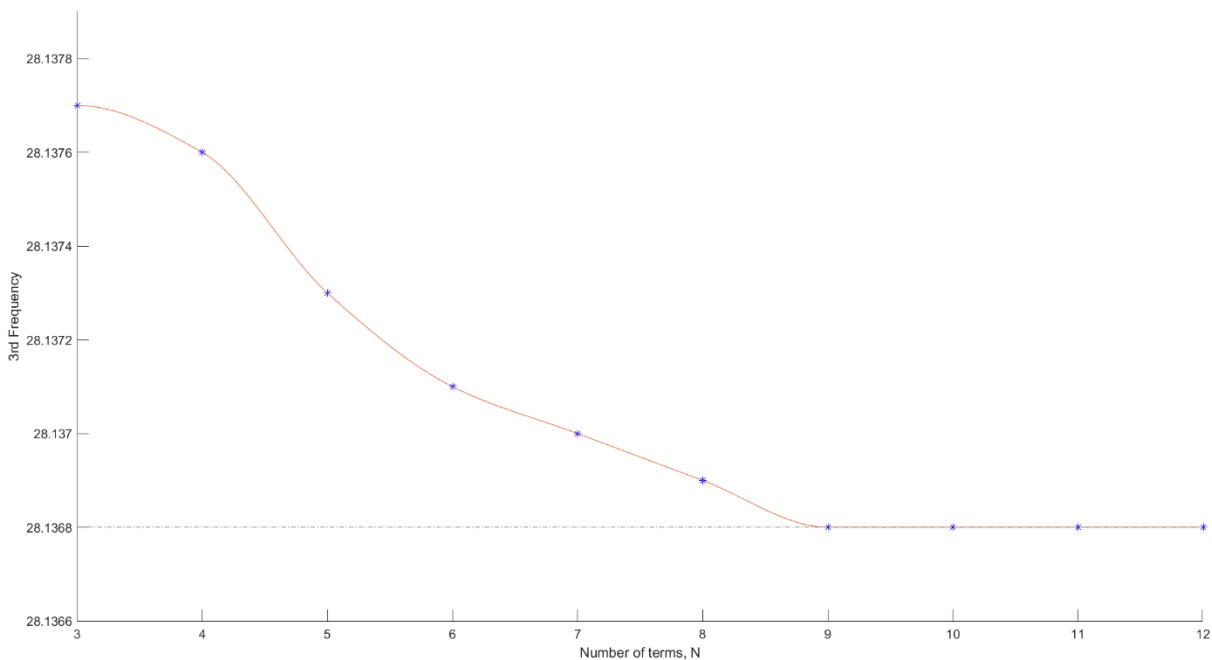


Figure 8. Convergence plot of Number of terms (N) vs 3rd Frequency.

From the convergence graph above, we see that the results approach to a stagnant value at the frequency of **28.1368 Hz** right from the point where N = 9. Hence, it suggests that we must have at-least 9 terms included in the shape function.

IV.C Pressure-load condition effect

A yet another objective of this vibration analysis is to see how pressure conditions develop over the wing surface. A large negative or positive pressure over the wing, anywhere in the mid-chord length region may introduce new set of calculations for the wing vibration. We would then need to include the uniformly varying pressure load as one of the dynamic boundary conditions in the equation of motion. If pressure load is established due to flow characteristics over a wing surface, there may also be an additional damping term added in the equation of motion. Then the equation of motion with damping D_s would become;

$$M_s \ddot{\underline{r}}(t) + D_s \dot{\underline{r}}(t) + K_s \underline{r}(t) = B_f \cdot \underline{f}(t)$$

Since damping is introduced not from the boundaries of the wing, we would need to design our variables, i.e. $u(x,t)$, again such that it now also includes pressure loads in the parameters involved. Moreover, the CFD simulation result also indicates that involving the pressure-based loads is not necessary since the pressure wave is getting established much farther than the concerned region (at $\sim 89 - 90\%$ of chord length). The contour graph below evidences it;

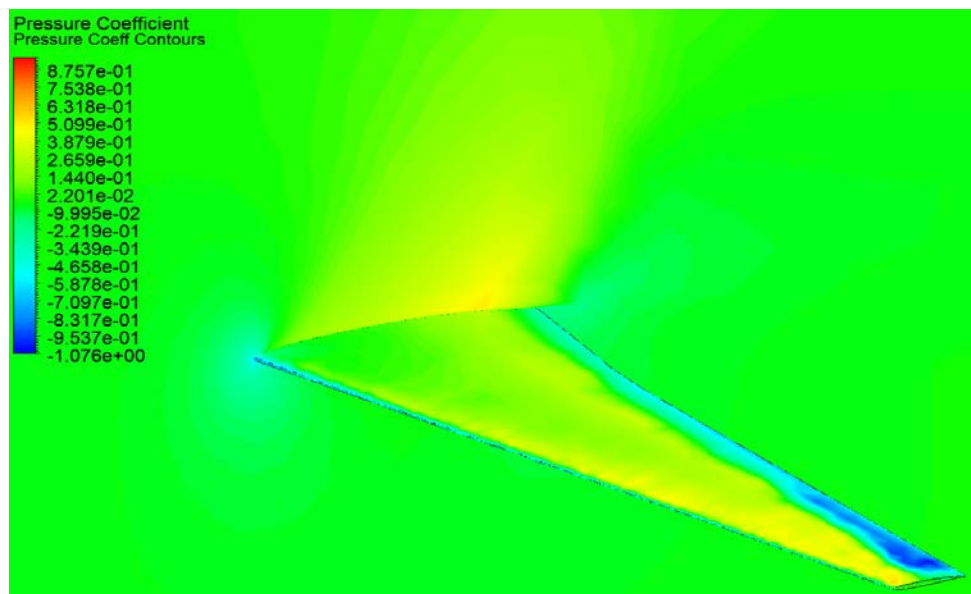


Figure 9. Pressure coefficient contours suggesting high density regions in yellow

V. RESULTS

The two methods, namely ANSYS FE analysis and Analytical computation were different in the sense that one used a direct replicated virtual model and performed analysis on it, while the other was more of a mathematical modelling scheme. The results obtained from analytical computation were only in agreement for the 1st frequency value. For the rest two frequencies, the values were significantly higher when compared to respective values from ANSYS FEA modal results. The error is reported below;

Table 5. Tabulation of error among the frequency values arrived from both the methods

Frequency	ANSYS FE Method	Analytical method	Absolute Error in result
f_1	1.4611	1.6035	9.74 %
f_2	3.9516	10.0488	154 %
f_3	8.1431	28.1368	71.1 %

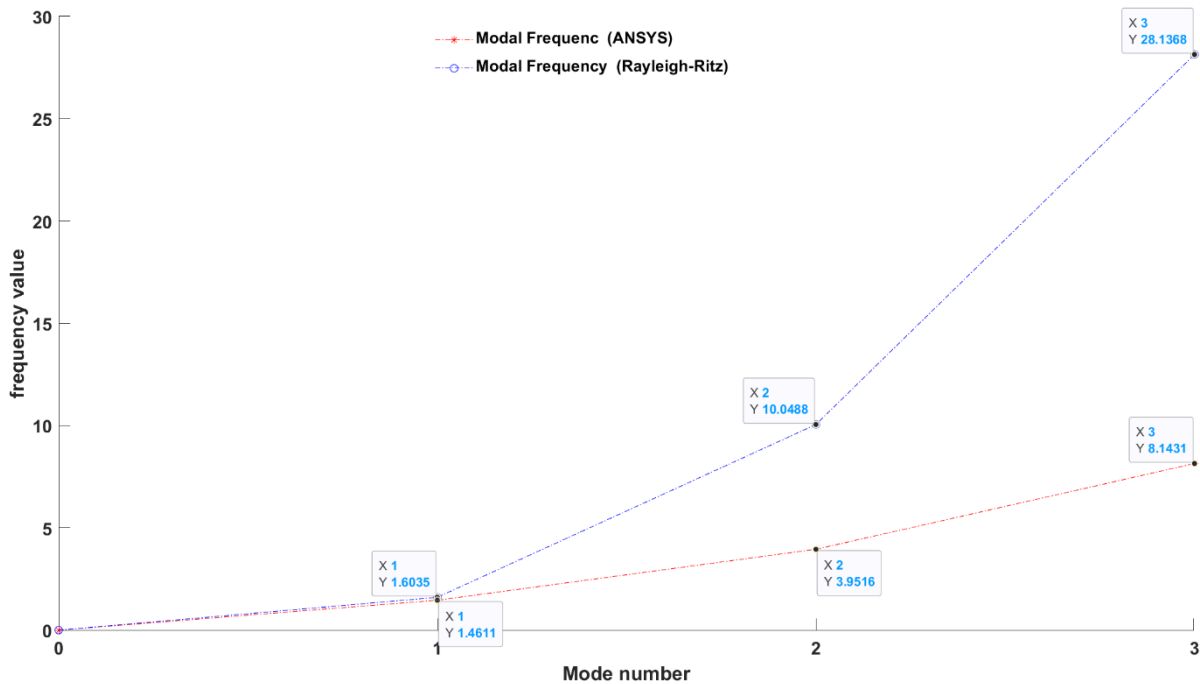


Figure 10. Frequency trend of the three modes of vibration for both the methods

The highlighted 1st frequency value is in good agreement with both the methods. The reason for large errors in 2nd and 3rd frequency can be because of incomplete and inadequate design attributes in the 3D model description and in the mathematical modelling.

In this analysis, many assumptions and simplifications have played a great role. The analysis was started with Finite Element Analysis using ANSYS where the wing model inputted was a simply drafted CAD geometry constructed out of the drawing views of Airbus A380-800. This hides the effects of all the individual interacting elements. The way they are constrained in the overall wing structure is also crucial from engineering analysis point-of-view. Then, we switched to analysis using analytical numerical method in MATLAB, where we simply assumed that our wing, being a cantilever-like structure can be approximated as a rectangular

cantilever beam-like structure. Therefore, the shape details cannot be modelled appropriately in the MATLAB analysis method. A yet another shortcoming of this analytical analysis was computation accuracy and resultant time. It was observed that with higher number of terms in the mode shape, the integration resulted in better answers. However, it drastically affected the time taken to deliver the results. With each increasing number of terms, the size of M_s & K_s blocks are increasing several folds. The analytical way uses an in-built integration function - '*integral3*'. This function uses Riemann sum; an integral approximation which uses finite element sum. Since Riemann sum is a kind of discretization process, it is incurring higher amount of calculation time with larger dimensions of M_s & K_s matrices.

A complete free-vibration analysis would demand that true flight conditions be emulated and vibrating natural frequencies at which the whole wing structure resonates be recorded. Nonetheless, it can be reasonably said that these simplifications and assumptions work well when performing a non-standard computer-based simulation test.

V. CONCLUSIONS

Overall, this project was a good opportunity to understand the dynamics of free-vibration problem. The wing of the chosen aircraft model was believed to appertain from supercritical air-foil profile series which was validated by fluid-flow simulation using ANSYS CFD. The aircraft wing being the substrate was approximated as a cantilever beam whose vibration characteristics were determined using ANSYS FE analysis, and later an analytical method given by Rayleigh-Ritz was implemented to validate the results with that of ANSYS FEA. The investigation revealed that the values of 1st modal frequency at which the whole wing would naturally vibrate were of the same tune from both the methods. However, the subsequent 2nd and 3rd modal frequencies were resulted out-of-tune with a high magnitude of error. This points at the assumptions and simplifications which were a part of this study.

The applicability of analytical computation methods like Rayleigh-Ritz approximation is guaranteed by a near correct 1st frequency value of the mode. It was proved that including larger number of terms improves the results and make them converge to a higher accuracy. A large number of terms would mean that the same shape function would get superimposed again and again for the desired number of times, hence closing-up to the desired. But involving large number of terms has direct effect on computation time. We can work on creating a robust goal-seeking algorithm which is time efficient. Also, there needs to be more refinement in the design and parameterization in order to justifiably represent such life-size aircraft wing given all the structural complexities that lies in it.

VI. REFERENCES

- [1] R. Roedts, R. Somero and C. Waskiewicz. [Online]. Available: http://www.dept.aoe.vt.edu/~mason/Mason_f/A380Roedts.pdf.
- [2] P. T. Karnick and K. Venkatraman, "Shock and boundary layer interaction and energetics," *Journal of Fluid mechanics*, p. 215, 2017.
- [3] D. J. Inman, *Engineering Vibrations*, Pearson Education, Inc, 2014.
- [4] S. Rao, *Mechanical Vibrations*, Pearson Education Limited, 2011.
- [5] J. Jaworski and E. Dowell, "Free vibration of a cantilevered beam with multiple steps:," *Journal of Sound and Vibration*, 2007.
- [6] G. M. OOSTERHOUT, P. J. M. V. D. HOOGT and R. M. E. J. SPIERING, "ACCURATE CALCULATION METHODS FOR NATURAL FREQUENCIES OF PLATES WITH SPECIAL ATTENTION TO THE HIGHER MODES," *Journal of Sound and Vibration*, 1994.
- [7] AIRBUS S.A.S., "AIRCRAFT CHARACTERISTICS - AIRPORT AND MAINTENANCE PLANNING," 30 March 2005. [Online]. Available: www.airbus.com.
- [8] G. Caminha, "The CFL Condition and How to Choose Your Timestep Size," 17 October 2019. [Online]. Available: <https://www.simscale.com/blog/2017/08/cfl-condition/>.
- [9] R. L. Pastel, J. E. Caruthers and W. Frost, "Airplane wing vibrations due to atmospheric turbulence," NASA, Washington, United States, Tullahoma, 1981.